

**THE CONTRIBUTION OF TYROSINE  $\Rightarrow$  WATER HYDROGEN  
BONDS TO PROTEIN STABILITY**

A Senior Thesis

by

CHARLES JOHN BECHERT

Submitted to the Office of Honors Programs and Academic Scholarships of  
Texas A&M University  
in partial fulfillment of the requirements for

1998-99 UNIVERSITY UNDERGRADUATE RESEARCH FELLOWS PROGRAM

April 1999

Fellows Group: Chemistry  
Major Subject: Biochemistry

**THE CONTRIBUTION OF TYROSINE  $\Rightarrow$  WATER HYDROGEN  
BONDS TO PROTEIN STABILITY**

A Senior Thesis

by

CHARLES JOHN BECHERT

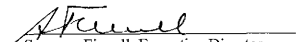
Submitted to the Office of Honors Programs and Academic Scholarships of  
Texas A&M University  
in partial fulfillment of the requirements for

1998-99 UNIVERSITY UNDERGRADUATE RESEARCH FELLOWS PROGRAM

Approved as to style and content by:



C. Nick Pace  
(Faculty Advisor)



Susanna Finnell, Executive Director  
Honors Programs and Academic Scholarships

April 1999

Fellows Group: Chemistry  
Major Subject: Biochemistry

**ABSTRACT****The Contribution of Tyrosine  $\Rightarrow$  Water Hydrogen Bonds to Protein Stability. (April 1999)**

Charles John Bechert, University Undergraduate Fellow, 1998-1999, Texas A&M University, Department of Biochemistry and Biophysics  
Faculty Advisor: Dr. C. Nick Pace

The goal of this research was to determine how protein stability is affected when tyrosines form specific inter and/or intramolecular hydrogen bonds in the folded state. Our model protein, the enzyme RNase Sa, contains four Tyr residues believed to form one or more intermolecular hydrogen bonds to surface or partially buried water molecules. To study these interactions the single mutants Tyr 30, 49, 55, 81 $\rightarrow$ Phe were prepared and their conformational stability and thermodynamics of folding analyzed. From thermal denaturation data the free energy of unfolding,  $\Delta G_U$ , enthalpy of unfolding,  $\Delta H$ , the melting temperature,  $T_m$ , and heat capacity change associated with unfolding,  $\Delta C_p$ , have been calculated. Initial analysis of Tyr 30, 49, 55, 81 predicted that each residue formed hydrogen bonds to one or more water molecules; however, thermodynamic and NMR data from this study support the surprising results that Tyr81 appears to establish an atypical intramolecular bond contributing 1.2 Kcal/mol to stability. Data for Tyr 30, 49, 55 support the prediction that intermolecular hydrogen bonds to water molecules are formed.

DEDICATION

To my friends and family,  
for their love and support

## ACKNOWLEDGMENTS

Special thanks to Kevin Shaw and David Schell for their enduring support, knowledge and discussions and to Dr. Pace for making it all possible. I wish to express my appreciation to Dr. Scholtz and to all the people in the Pace and Scholtz labs that have helped me at one time or another. I also owe a debt of gratitude to lab predecessors, especially Eric Herbert, who developed much of the system and protocols used in this research.

## TABLE OF CONTENTS

	Page
ABSTRACT .....	iii
DEDICATION .....	iv
ACKNOWLEDGMENTS .....	v
TABLE OF CONTENTS .....	vi
INTRODUCTION .....	
The Protein Folding Problem.....	1
Hydrophobic Effect.....	4
van der Waals Interactions.....	5
Electrostatic Interactions.....	7
Hydrogen Bonding.....	7
Description of the Project.....	9
The Experiment .....	12
METHODOLOGY .....	13
Oligonucleotides .....	14
Site-Directed Mutagenesis.....	14
Enzymatic Manipulations .....	16
Expression System, Media and Growth Conditions .....	16
Protein Purification .....	17
Chromatography and SDS gel .....	18
Enzyme Activity .....	18
Circular Dichroism Spectra.....	19
RESULTS .....	20
DISCUSSION .....	25
CONCLUSION .....	29
REFERENCES .....	30

## INTRODUCTION

### *The Protein Folding Problem*

A long-standing problem in science has been the question of what makes proteins fold. What causes linear amino acid sequences to fold into complex three-dimensional structures. The protein folding problem was recognized by Mirsky and Pauling, (1936). Subsequently, it was first shown by Anfinsen et al. in 1961 that all of the information needed for ribonuclease-A to fold into its native conformation is coded in its amino acid sequence alone. Although early discussions of protein structure revolved around the hydrogen bond (Pauling and Corey, 1951) by the 1960s the work by Kauzmann (1959) and Tanford (1962) shifted the emphasis to hydrophobic interactions as the single most dominant force driving the protein to fold into its native conformation. A third stabilizing factor in many naturally occurring proteins is the covalent cross-links resulting from the formation of the disulfide bonds between cysteine residues. Other factors that are smaller in their absolute strengths, but probably equally important in their influence, are van der Waals interactions, ion-pairs, aromatic-aromatic interactions, helix-dipole and so on (Dill, 1990). The single most important force favoring the unfolding of a protein is entropy.

Primary structure is now perhaps the easiest to ascertain, for it can be learned by either sequencing its messenger RNA or by chemically breaking the protein down residue by residue, and identifying each piece. To determine what secondary structure a chain might fold into, the sequence is compared to other solved-structure sequences to determine if any residue similarities exist, and if so, then their folding can be predicted. For example, an amino acid sequence that has hydrophobic side chains every three or four residues may be interpreted as a set of straight helices that wrap around a complementary hydrophobic area. However, divination of structure is not certain, for some sequences fold both into sheets and helices, all depending on their tertiary environment. By continuing this study of structure, it is possible to compare proteins by entire sequences.

Protein homology information can be used to approximate unknown tertiary structures. The idea is that through past mutations two copies of a protein that once arose by gene duplication will in time diverge from each other. In general, the hydrophobic core of a protein tends to be conserved, as most mutations will tend to make it more unstable, by disrupting bonds and packing, exposing the core to water. On the exterior, matches between two proteins hydrophilic and neutral amino acids will be small, as many amino acids have nearly the same affinity for water, and mutations, or genetic drift, may occur without consequence. With this knowledge, a protein with an unknown tertiary structure may be entered in a sequence database, akin to secondary structure, and scanned for similarities. Related proteins need to be only about thirty percent conserved to be similar in their tertiary structures. So if a match does occur, a rough description of the protein may be extrapolated. However, often a new amino acid sequence does not match the limited set of solved structures, and so other techniques must be used to determine the structure. One such method is x-ray crystallography, in which radiation is diffracted through an ordered lattice of proteins to determine their structures. The imaging of a protein's structure by x-ray crystallography is analogous to a conventional light microscope, in which both focus diffracted light with a lens by scattering x-rays off a protein crystal, the scattering of the x-rays is observed from the interference and reinforcement of the radiation. With considerable effort, this is recombined into an electron density map by either a computer or a human. However, many complications often prohibit crystallography. Proteins are very difficult to crystallize due to their aqueous nature and irregular shape, and each crystal has its particular concentrations of buffer, ions, and pH required to crystallize. Once accomplished, the packing of the crystal might not be tight enough to give a high enough resolution for a sharp map. And portions of the information carried by the diffracted light are undetectable, and must be recalculated for each of the several thousand atoms present. Overcoming these limitations is possible, but they have restricted researchers to solve less than one structure per twenty known protein sequences.



A second tool in determining a protein's structure is the use of magnetic fields to determine an atom's neighbors. Called nuclear magnetic resonance (NMR), a picture of all the environments that hydrogen atoms are in inside the molecule can be obtained by using just milligrams of very pure protein. The atoms are subjected to varying fields and, depending on their environments, resonate each at a particular frequency. From this, neighboring atoms can be determined, in sequence as well as in space, and a three-dimensional model can be created. However, limitations arise as the frequency data tends to blur together with an increasing number of residues, so NMR tends to be useful with smaller proteins. Evidence gathered using a variety of spectroscopic techniques (NMR, CD and UV) supports the hypothesis of a rapid collapse of the denatured peptide to a fold which is closely related to the native fold, known as the molten globule, in which hydrophobic residues are sequestered to the interior of the globule. Recent stopped flow 2D competitive hydrogen exchange NMR has produced evidence for an analogous but more transient early folding intermediate in the T4 and the hen egg white-like lysozymes (Miranker et al., 1991).

By studying proteins, scientists hope to gain insight into how modifying the amino acid sequence might be utilized in creating new drugs, modifying existing structures or altering their stability. Knowledge of protein stabilizing interactions is essential for better understanding of proteins like prions, for which the 1997 Nobel Prize in Physiology or Medicine was awarded to Stanley Prusiner. He discovered that prions possess an innate capacity to convert their structures into *highly stable* conformations that ultimately result in the formation of harmful proteins that cause several deadly brain diseases (Prusiner, 1995). A protein's unique folded conformation is maintained by a combination of forces. The most important stabilizing forces are hydrogen bonds and hydrophobic repulsion. These forces are opposed by entropy, the most important destabilizing force. For a protein's native structure to be stable, the summation of the bonding interactions for the native state must have a lower free energy than for the denatured state.

Protein structural equilibrium is usually described by the following expression,



Where  $N$  represents the Native or folded state and  $D$  represents the denatured or unfolded state. The conformational stability of a folded protein is defined as the difference in the free energy,  $\Delta G_U$ , between the native and denatured states:

$$\Delta G_U = G_D - G_N$$

$\Delta G_U$  is positive for a protein that is stable under particular conditions. For most globular proteins under physiological conditions, the native state is only 5-10 kcal mol<sup>-1</sup> more stable than the denatured state (Pace, 1975). Protein stability depends on the free energy change between the folded and unfolded states which is expressed by the following,

$$-RT \ln K = \Delta G = \Delta H - T \Delta S$$

where  $R$  represents the gas constant,  $K$ , the equilibrium constant,  $\Delta G$ , the free energy change.  $\Delta H$ , the enthalpy change and  $\Delta S$ , the entropy change between the folded and unfolded conformations. The enthalpy change,  $\Delta H$ , corresponds to the binding energy (dispersion forces, electrostatic interactions, van der Waals potentials and hydrogen bonding) while hydrophobic interactions contribute mainly to the entropy term,  $\Delta S$ .

### *Hydrophobic Effect*

Kauzmann was first to elucidate the importance of the hydrophobic effect based on analyses of thermodynamic data that characterized the transfer of nonpolar solutes from water to nonpolar solvents (Kauzmann, 1959). Proteins, upon folding, have about 80% of their nonpolar hydrophobic surfaces buried in the interior. The burial results from nonpolar atoms having an affinity for a nonaqueous environment and that described as the hydrophobic effect. Quantitative estimates for the hydrophobic effect in proteins are usually made by measuring the  $\Delta G_{tr}$  (transfer) values of the amino acid side chains into various nonpolar solvents, detergent micelles or the vapor phase (Tanford, 1962) that model the protein interior. The  $\Delta G_{tr}$  values for the nonpolar side chains in these model

solvents are positive, indicating that they prefer a nonpolar nonaqueous environment. At room temperature this unfavorable transfer results from an unfavorable change in the entropy of the system that is thought to occur due to increased ordering of water molecules around the nonpolar side chain needed for solvation (Kauzmann, 1959).

In order to gain a better understanding of the contribution of burying nonpolar residues in the interior of a protein, experimental studies of the hydrophobic effect using site-directed mutagenesis were reviewed and analyzed for a large set of mutants in several different proteins (Pace, 1992). It was determined, from 72 hydrophobic mutants of these studies, that burying a  $-CH_2-$  in the interior of the protein on average contributes  $\sim 1.3$  kcal mol<sup>-1</sup> to the stability of a protein (Pace, 1992). The measured  $\Delta(\Delta G)$  values for these mutants have a large variation and were substantially larger than the  $\Delta G_u$  values expected if n-octanol data was used to model the protein interior.

To maximize van der Waals interactions a protein packs in such a way that its hydrophobic interior closely resembles the packing density seen for crystals (Chothia, 1984). One study's results suggests that for the mutants in T4 lysozyme, some of the variation is due to the loss of van der Waals contacts produced by creating a cavity in the protein (Ericksson et al. 1992). These researchers crystallized seven Leu→Ala and Phe→Ala mutants in T4 lysozyme discovering that in every mutant, slight conformational rearrangements around the site of the mutation reduced the cavity size left by the mutation, but in all cases a cavity still remained; therefore, if the dependence of the measured  $\Delta(\Delta G)$  value on cavity size is extrapolated back to zero cavity size, the measured  $\Delta(\Delta G) \cong \Delta G_u$  values measured in n-octanol, a conclusions supported by the theoretical calculations and model compound data in a study by Lee, (1993).

#### *van der Waals Interactions*

van der Waals interactions involve relatively weak forces that are one to three orders of magnitude weaker than covalent forces. Despite this fact, the large number of these weak interactions create a sizable interaction energy (Maitland et al., 1981). These weak forces come from the uneven distribution or polarization of electrons in relation to the nucleus that creates a transient dipole. This dipole in turn distorts the electron shell of a neighboring atom, resulting in dipole coupling or oscillating dipoles that generates an

attractive force such that all atoms can attract each other even in the absence of formal charges. The attraction results from interactions involving the polarization of the electron field of one atom in the presence of another. The strength of these interactions, often called dispersion forces or London forces, depends on the distance between the dipoles and the polarizability of the atoms (Maitland et al., 1981). Calculating the attractive force,  $E_a$ , can be approximated using the inverse sixth power of the separation distance,  $r$ , between the two atoms, where  $C_6$  is a coefficient that depends on polarizability and ionization constants of the atoms (Maitland et al., 1981).

$$E_a = \frac{C_6}{r^6}$$

van der Waals interactions also include repulsive forces between atoms that are the most important and strongest noncovalent interactions between two atoms. Atomic repulsion increases steeply as the separation distance between the two atoms decreases due to the overlap between the atomic electron orbitals (Maitland et al., 1981). Calculating the repulsive energy,  $E_r$ , can be approximated using the equation below, where  $C_n$  is a coefficient that depends on the identity of the atoms (Maitland et al., 1981).

$$E_r = \frac{C_n}{r^n}$$

Van der Waals interactions can also be represented by the Lennard-Jones 12,6 potential which includes both the repulsive and attractive terms. The value  $n = 12$  is commonly used in the repulsive term for computational efficiency (Maitland et al., 1981).

$$E_{vdw} = \frac{C_{12}}{r^{12}} - \frac{C_6}{r^6}$$

### *Electrostatic Interactions*

In proteins, charges are not simple point charges. Charges on the side chains of Arg, Lys, His, Asp, Glu, and the  $\alpha$ -amino and  $\alpha$ -carboxyl groups are localized around atoms or are distributed over groups of atoms. Additionally, the use of the dielectric

constant in Coulomb's law is only valid for a homogeneous environment (Feynman et al., 1977). In a vacuum, Coulomb's law states that the energy of interaction,  $E_C$ , between two point charges,  $q_1$  and  $q_2$ , separated by a distance,  $r_{12}$ , is given by (Feynman et al., 1977). For charges of opposite sign, the

$$E_C \propto \frac{q_1 q_2}{r_{12}^2}$$

interaction energy is attractive and increases as the separation decreases, whereas for like charges the interaction is repulsive. Coulomb's law is only valid for point charges in a vacuum and must be modified when the point charges are in other environments. In a homogeneous liquid such as water, the electrostatic interaction decreases as the polarity of the environment increases, and this dependence is accounted for by incorporating the dielectric constant,  $D$ , for the medium.

$$E_{\epsilon, l} \propto \frac{q_1 q_2}{D r_{12}^2}$$

A salt bridge is a specific ion pair in which hydrogen bonding interactions between the charged groups are also present. In many proteins, specific ion pairs have been shown to account for large portions of the net stability. For example, a strong ion pairs is in T4 lysozyme: residues Asp70 and His31 which form an ion pair with a measured contribution to the free energy of folding of 3-5 kcal mol<sup>-1</sup> (Anderson et al., 1990).

### *Hydrogen Bonding*

The interaction energy for hydrogen bonds is mostly due to electrostatic and charge transfer effects, but exchange repulsion, polarization, and coupling also make important contributions (Umeyama and Morokuma, 1977). Hydrogen bonds can be classified into four general categories: main chain ↔ main chain, main chain ↔ side chain, side chain ↔ side chain interactions, or for surface groups, hydrogen bonds with the external solvent. Hydrogen bonds may individually make only small contributions to the free energy of stabilization of the structure, but their importance is shown by studies

on the heat stability of proteins which suggest that the addition of only a very few hydrogen bonds, ion pairs or other stabilizing interactions can dramatically increase stability and resistance to heat denaturation. Within proteins all groups that are capable of hydrogen bonding, do so. Main chain groups are most often hydrogen bonded to each other while local side chain- main chain interactions help to satisfy the hydrogen bonding potential of free NH groups in beta turns and at the N -termini of helices. The structural role of C=O groups is influenced by their preference for two hydrogen bonds.

Water molecules play valuable structural roles by forming hydrogen bonds with a protein groups that are not in close proximity with an intramolecular group. Generally, O-H-O hydrogen bonds are stronger than N-H-O hydrogen bonds, resulting from increased polarization of the hydrogen atom due to the larger electronegativity of the oxygen donor. Additionally, hydrogen bonding interactions involving charged groups, like the positively charged side chains of lysine or arginine, are generally stronger than those involving neutral polar groups (Fersht et al., 1985).

As acceptors, C=O and -O- are the most common, with minor contributions from -N= and -S-. The >N-H and >C=O groups in the peptide bond are the most important hydrogen bonding groups in proteins, but the side chains of Asp, Arg, Asn, Cys, Gln, Glu, His, Lys, Ser, Thr, Tyr and Trp contain polar atoms and are capable of forming one to five hydrogen bonding interactions (Baker & Hubbard, 1984).

TABLE-2 Provides  $\Delta(\Delta G)$  values for 32 Tyr to Phe mutants in eight proteins that on average have hydrogen bonds that contribute  $1.15 \text{ kcal mol}^{-1}$  to protein stability (Pace, unpublished observations). In addition to protein hydrogen bonding, peptide hydrogen bonding was estimated to contribute about  $1 \text{ kcal mol}^{-1}$  to helix stability (Scholtz et al., 1991). Individual peptide units are relatively rigid. The degrees of freedom available for folding the peptide chain are rotations around the  $C\alpha$ -C' bond, described by the angle  $\phi$ , and around the N-C $\alpha$  bond,  $\psi$ . The angles which can be adopted by these bonds are restricted by steric interactions of the amino acid side-chains (Ramachandran and Sassiexharan, 1968).

### *Description of the Project*

The primary goals of this research are to gain a better understanding of the forces that contribute to the conformational stability of globular proteins, and subsequently to gain insight into the mechanism of folding. Achieving these goals requires a thorough understanding of the structures of the folded and unfolded conformations of proteins and of the effect of changes in structure on the equilibrium between these states. The research proposed here will focus on RNase Sa because it has features that make it nearly ideal

for the planned studies: for example, it is the smallest member of the microbial RNase family, with just 96 amino acids. Recently, a 1.2 Å resolution structure has been determined at room temperature and a 1.0 Å structure has been determined at 70 °K (Sevcik et al., 1996). RNase Sa is an extra-cellular ribonuclease isolated from *Streptomyces aureofaciens* (Gasperik et al., 1982). The enzyme contains one disulfide bond, with no methionine, lysine, or tryptophan residues. The enzyme catalyzes the cleavage of single-stranded RNA preferentially after guanosine residues producing nucleotides with a 3' phosphate (Zelinkova, 1971). The catalytic mechanism of RNase Sa has been examined through a series of X-ray crystallographic studies by Sevcik and his collaborators (Sevcik et al., 1996).

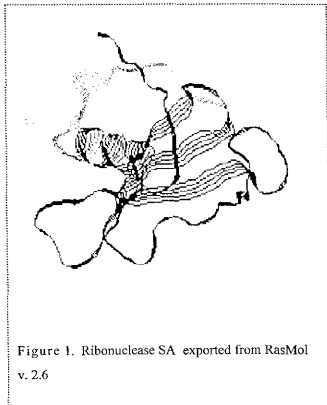


Figure 1. Ribonuclease SA exported from RasMol v. 2.6

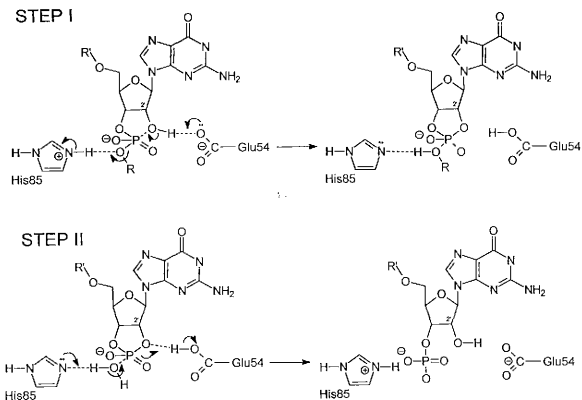


Figure 2. Catalytic mechanism of RNase Sa (Findlay et al., 1961)

The catalytic mechanism of RNase Sa involves two steps, transesterification and hydrolysis. This acid/base mechanism of cleavage was first proposed by Findlay (Findlay et al., 1961) and involves a transesterification that results in the formation of a 2',3'-cyclophosphate intermediate (STEP I). His85 interacts with oxygen changing the PO bond angles thereby creating a disruption of the negative electron shielding normally surrounding the phosphorus atom. Subsequently, the atom is open to nucleophilic attack. The Glu54 base abstracts a proton from the O<sup>2'</sup> of the ribose sugar resulting in an anion that engages in the nucleophilic attack on the phosphodiester linkage to yield a pentavalent phosphate intermediate. The catalytic acid His85 donates a proton causing departure of the leaving group, ROH. In the hydrolysis STEP II, the acid/base catalytic roles of Glu54 and His85 are reversed. His85 abstracts a proton from a water molecule, causing the water to nucleophilically attack the cyclophosphate intermediate, resulting in Glu54 donating a proton to O<sup>2'</sup>. Hydrolysis of the 2',3'-cyclophosphate intermediate has



been shown to occur through an in-line mechanism (Eckstein et al., 1972), resulting in the formation of 3'-guanosine nucleotide.

RNase Sa contains 8 Tyr residues, of which four of the Tyr residues studied previously all form one intramolecular hydrogen bond and one hydrogen bond to a water molecule. The other four Tyr residues appear to form hydrogen bonds to only water molecules. Tyr 30 and 81 form hydrogen bonds to a single water molecule, and Tyr 49 and 55 form hydrogen bonds to two water molecules (Pace et al., 1998). The typical goal in studying hydrogen bonding mutants is to learn how much stability is gained when a polar group that is hydrogen bonded to water in the unfolded state is dehydrated to form a specific intramolecular hydrogen bond in the folded state. The most common approach has been to replace a side chain involved in a hydrogen bond, such as Asn, with a side chain that cannot form a hydrogen bond, such as Ala. Asn residues are generally more exposed to solvent than nonpolar residues and they form up to four intramolecular hydrogen bonds. An amide group is capable of forming four hydrogen bonds, two as a donor and two as an acceptor (Stickle, 1992.) Previous studies indicate that the mutant is less stable than the wild-type protein although an Ala side chain is more hydrophobic than an Asn side chain by  $\sim 1.2$  kcal/mol. This suggests that the loss of the hydrogen bonds contributes more to the  $\Delta(\Delta G)$  value than the gain from the increase in hydrophobicity (Pace et al. 1996.) The  $\Delta(\Delta G)$  values resulting when a given hydrogen bonding group is removed by mutation will depend on the bond angle and bond length, on the groups that participate, and on the location of the hydrogen bond in the protein. In addition, the  $\Delta(\Delta G)$  value will depend on what happens to the remaining member of the hydrogen bonding pair in the mutant protein. In the most favorable case, the remaining member of the hydrogen bonding pair forms a hydrogen bond to a water molecule in the mutant protein, in this case,  $\Delta(\Delta G)$  will depend on the number of hydrogen bonds removed and will give us the information sought. Alternatively, if the remaining partner forms a new intramolecular hydrogen bond, then  $\Delta(\Delta G) \approx 0$  would be expected; but if the partner is left unpaired, then a large negative  $\Delta(\Delta G)$  value would be expected because the partner will form hydrogen bonds with water in the unfolded protein.



Figure 3. (left) Four Tyrosine residues of the RNase SA native structure that were modified to form four different mutant structures with phenylalanine substituted in place of the tyrosine. (right) RNase SA structure depicting all 4 mutations rendered in ball and stick format with molscript (Kraulis, 1991).

### *The Experiment*

Therefore, to further gain an understanding of the contribution of the burial and hydrogen bonding of Tyrosine side chains to protein stability, the following single mutants were prepared and their conformational stability and thermodynamics of folding studied: RNase Sa (Tyr 30, 49, 55, 81  $\rightarrow$  Phe). Studying the RNase Sa mutants will allow us to compare the importance of intramolecular hydrogen bonds involving other groups within the protein versus intermolecular hydrogen bonds involving buried  $H_2O$

molecules. By measuring the difference in stability between the mutant and the wild-type protein, that is  $\Delta(\Delta G)$ , one hopes to gain insight into the contribution of hydrogen bonding to the stability of the protein, and a better understanding of the importance of protein hydration to protein stability may be gained. Additionally, this information will help theoreticians improve the methods they use for modeling the contribution of electrostatic and van der Waals interactions to protein stability. This study will provide a better understanding of the effect of changes in the amino acid sequence on the structure of the folded and unfolded conformations of proteins, and of the mechanism of folding and of the forces that stabilize the folded conformation of globular proteins. This basic information will prove to be valuable in designing and preparing novel proteins for medical and biotechnological applications.

## METHODOLOGY

Below is a flow chart sequence, followed by details, that is a concise overview of the reasonably well established molecular biology and biochemistry techniques that were employed.

### METHODOLOGY OVERVIEW

Oligonucleotide design → Site-directed mutagenesis →  
PCR → Ligation → Transformation-1 →  
DNA extraction / sequencing → Transformation-2 →  
Protein expression → Protein purification → SDS PAGE gel  
Protein analysis by thermal denaturation with CD spectroscopy

### Oligonucleotides

Oligonucleotides were made at the 40 nanomolar scale on a polystyrene support matrix using phosphoramidite chemistry and dimethyltrityl protection chemistry on either an Applied Biosystems Inc., 391, 380B, or 394 DNA synthesizer by the Gene Technologies Laboratory, Texas A&M University (College Station, Texas). Concentration of oligo-nucleotide stocks were measured on a Hewlett Packard Spectrophotometer using a 1 cm cuvette and an absorption coefficient for single-stranded DNA of  $0.05 \text{ mg}^{-1} \text{ ml cm}^{-1}$ .

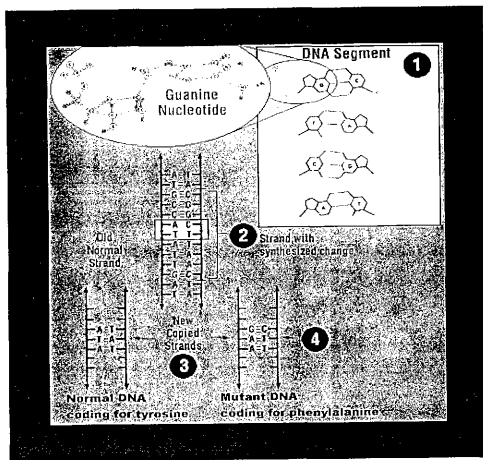


Figure 4. Overview of site-directed mutagenesis.

### Site-Directed Mutagenesis

RNase Sa Mutants were constructed using the four primer polymerase chain reaction (PCR) overlapping extension technique (Ho et al., 1989). Three separate reactions were required for each mutant. The first and second reactions produced the 5'

and 3' ends of the gene and incorporated a mutated primer in each. The final reaction results in the complete amplification of the altered sequence. Included in a 100 ml PCR reaction volume is 3.20 pmol each primer, 10 ng pEH100, 200 mM dNTPs, and 2.5 U Vent polymerase. A typical thermal cycler profile is 95 °C (1.5 minutes), 72 °C (2 minutes) for 1 cycle, followed by 25 cycles of 90 °C (45 seconds), 72 °C (1.5 minutes), and then a 7.0 minute extension period at 70 °C. Samples were frozen at -20 °C until needed. PCR products were analyzed by running 5 ml of the reaction on a 1.5 or 2% agarose gel (0.5X TBE, 0.25 mg/ml ethidium bromide).

The final PCR product, insert DNA with desired mutation, was purified with the Qiagen PCR clean up kit. and digested with *Xba* I, precipitated with ethanol and then digested with *Eco*R I. The digested PCR insert was ligated with digested pEH101 vector yielding recombinant DNA. The recombinant DNA was then transformed into competent Nova Blue cells. The DNA was extracted from these recombinant organisms and sequenced to verify desired mutations. Finally this sequenced recombinant DNA is again transformed into competent cells for use in protein expression.

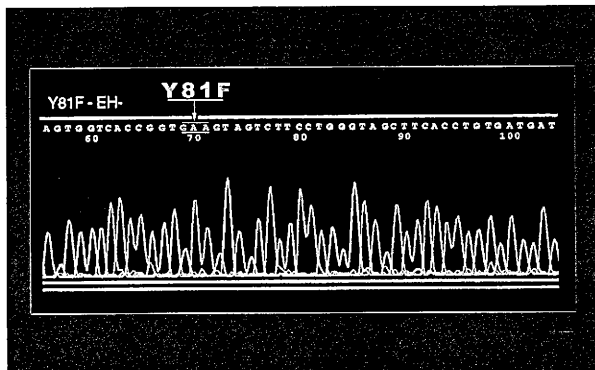


Figure 5. Actual sequencing for the Y81F mutant depicting the changed amino acids that will code for phenylalanine in place of tyrosine.

### *Enzymatic Manipulations & Gel Purification of DNA*

Restriction enzymes were used, as recommended by the manufacturer, Promega, Inc. to digest the plasmid DNA. Ligation of DNA fragments with T4 DNA ligase was performed as recommended by the manufacturer, Promega, Inc. Restriction digested vector DNA was purified using the Qiagen gel extraction kit.

### *Expression System, Media and Growth Conditions*

*E. coli* strain NovaBlue - Novagen, Inc., Madison, Wisconsin) were used as the host for the following plasmids: pEH100, and pEH101. Cells were grown at 30 °C in LB medium (10 g tryptone, 5 g yeast extract, 5 g NaCl per liter) or terrific broth medium (12 g tryptone, 24 g yeast extract, 4 ml glycerol, 2.31 g KH<sub>2</sub>PO<sub>4</sub>, 12.54 g K<sub>2</sub>HPO<sub>4</sub> per liter) containing ampicillin (25 mg/ml) and tetracycline (10 mg/ml). Plasmid DNA were isolated using the Qiagen miniprep kit from *E. coli* NovaBlue containing the desired plasmid and grown in 5 ml cultures of LB medium with antibiotics.

*E. coli* NovaBlue cells were made competent for DNA uptake using CaCl<sub>2</sub>. *E. coli* from a single colony inoculated into 50 ml of LB media containing 10 mg/ml tetracycline. Cells were grown to a OD<sub>600</sub> of 0.2, then incubated on ice for 20 minutes. Cells were then harvested by centrifugation in a Sorvall SS-34 rotor at 8,000 rpm for 10 minutes at 4 °C. The supernatant was discarded and the pellet re-suspended in 20 ml of ice-cold, filter sterilized 100 mM CaCl<sub>2</sub>. Cells were harvested as before and the supernatant discarded. The pellet was re-suspended in 2 ml of ice-cold, filter sterilized 100 mM CaCl<sub>2</sub> and 0.5 ml sterile 60% glycerol. Aliquots of 60 ml were transferred to sterile micro tubes and frozen at -80 °C.

For transformation, these cells were thawed and placed on ice for 10 minutes. DNA (~50-100 ng) was added and the cells were incubated for 20 minutes on ice. Cells were then heated to 42 °C for 90 seconds, followed by 2 minutes on ice. After the addition of 800 ml of LB media they were transferred to a 37 °C water bath for 45 minutes. Aliquots of the transformed cells were plated onto LB agar media containing antibiotics. The plates were incubated overnight at 30 °C.

### *Protein Purification & Cell Growth*

Transformed cells were grown overnight in 50 ml of LB medium, then diluted about 1:10 into 500 ml of terrific medium. This culture was grown at 30 °C to an OD<sub>600</sub> of 0.6, and subsequently diluted into 10.5 L of terrific broth medium in an 11 L benchtop fermentor (New Brunswick Scientific, Inc., Model 19). The culture was stirred at 250 rpm and aerated with filtered pressurized air at 12 L per minute. Growth was continued at 30 °C to an OD<sub>600</sub> of 0.6. At this point, RNase Sa expression was induced by the addition of IPTG to a final concentration of 0.1 mM. An additional aliquot of ampicillin (25 mg/ml) was also added at this time. Cultures were grown an additional 12 hours before harvesting.

RNase Sa was released from the periplasmic space of *E. coli* NovaBlue using an osmotic shock treatment. Cells were harvested in a Beckman JS-4.2 rotor at 4,000 rpm for 25 minutes. Cell pellets were resuspended by vigorous shaking in 2000 ml of 20% sucrose, 15 mM Tris pH ~7.4, 3 mM Na<sub>2</sub>EDTA and transferred to GSA bottles. After centrifugation in a Sorvall GSA rotor at 10,000 rpm for 30 minutes at 4 °C, the supernatant was saved and the cell pellets resuspended rapidly by vigorous shaking in 2000 ml of 15 mM Tris pH ~7.4, 3 mM Na<sub>2</sub>EDTA. After incubation for 20+ minutes on ice, cells were pelleted in a Sorvall GSA rotor as before and this supernatant was added to the first supernatant.

The combined supernatants (4000 ml of periplasmic fraction) were acidified by adding 10.8 g disodium succinate and 18.8 g succinic acid (final concentrations: 20 mM sodium/50 mM succinate). The final pH was adjusted to 3.25 with concentrated HCl and precipitate was removed by centrifugation in a Sorvall GSA rotor at 10,000 rpm for 15 minutes at 4 °C. The supernatant was stored at 4 °C until needed.

### *Chromatography and SDS gel*

C25 resin was pre-equilibrated with 1 L of 20 mM sodium/50 mM succinate buffer pH 3.25. After loading, the column was washed with 0.5 L of the low pH buffer. Elution was performed using a pH gradient from pH 3.25 to pH 6.0 in succinate buffer using a total volume of 1 L. Fraction volumes of about 15 ml were collected. All cation exchange chromatography runs were performed at room temperature. Fractions containing RNase activity were pooled and freeze dried.

The freeze dried RNase Sa sample from the ion exchange step was dissolved in a solution containing 3 ml of 2 M Tris pH 10.5 and 47 ml of 50 mM ammonium bicarbonate buffer (final pH ~7.0). The sample was eluted, from a G-50 Sephadex size-exclusion column, with 50 mM ammonium bicarbonate buffer pH 7.0. All G-50 runs were performed at room temperature. Fractions volumes of about 15 ml were collected. Fractions containing RNase activity were pooled and freeze dried.

Protein purity was examined by running the isolated proteins on 16%/3% Tricine SDS-PAGE. Gels were stained using standard Coomassie Brilliant Blue R-250.

### *Activity Assay*

Enzymatic activity for RNase Sa was measured using the basic techniques of Uchida and Egami. Five microliters of sample was added to 0.75 ml of 0.2 M Tris-HCl pH 7.5, 20 mM EDTA assay buffer. The reaction was initiated by adding 0.25 ml of a 12 mg ml<sup>-1</sup> solution of RNA (Torula Yeast or Baker's Yeast). After incubation for 15 minutes at 37°C, the reaction was stopped by adding 0.25 ml of uranyl reagent (0.75% uranyl acetate, in 25% perchloric acid (v/v)). Samples were incubated on ice for 10 minutes and centrifuged at 13,000 rpm for 6 minutes in a microfuge. Two hundred microliters of the supernatant was diluted into 5.0 ml distilled water and the  $A_{260}$  was measured against a blank consisting of the complete reaction mixture minus enzyme sample. When pooling active fractions for purification, fractions with a  $\Delta A_{260} < 0.4$  were excluded.



### *Circular Dichroism*

The thermal denaturation (Figure-6) of RNase Sa is followed by measuring the change in ellipticity at 234 nm using an Aviv 62DS Circular Dichroism Spectrophotometer. The temperature is increased from 5 to 80 °C in 1 °C increments with a 30 second equilibration time at each temperature. Typical results are shown in Figures 7-9 and summarized in TABLE-1. Measurements were made every 0.2 nm using a 1.0 nm bandwidth and a ten second time constant. Near UV spectra were measured in a 1.0 cm cuvette with a protein concentration of ~ 1.0 to 2.0 mg ml<sup>-1</sup>. All samples were measured in 30 mM NaMOPS at pH 7.0. Protein samples were filtered through a 0.2 mm Acrodisc syringe filter pre-equilibrated with 3 to 5 ml of buffer to remove any particulate material.

The thermal denaturation of RNase Sa proteins was followed by measuring the change in the CD signal at 234 nm with changing temperature. Protein solutions (0.05 to 0.15 mg ml<sup>-1</sup>, ~ 3 ml total solution volume, 30 mM buffer pH 7.0) were filtered using a 0.2 mm Acrodisc syringe filter pre-equilibrated with 3 to 5 ml of the same buffer. The change in ellipticity at 234 nm was recorded on an Aviv 62DS Circular Dichroism Spectrophotometer as the temperature increases from 5 to 80 °C by 1 °C increments with a 30 second equilibration time at each temperature. A band width of 1.0 nm and a time constant of 10 seconds were used.

## RESULTS

**TABLE 1.** Biophysical data characterizing the thermal unfolding of native RNase Sa and four hydrogen bonding mutants at pH 6.95 in 30 mM MOPS buffer.<sup>a</sup>

## T-MELT SET AVERAGE

<i>RNase Sa</i>	$T_m^b$	$\Delta T_m^c$	$\Delta H_m^d$	$\Delta S_m^e$	$\Delta G_U^f$
Sa-wt	48.6		95.5	297	
Tyr30→Phe	49.6	1.0	81.7	253	-0.30
Tyr49→Phe	47.6	-1.0	85.0	265	0.30
Tyr55→Phe	46.5	-2.1	92.0	288	0.62
Tyr81→Phe	44.5	-4.1	81.0	255	1.22

<sup>a</sup>  $T_m$  and  $\Delta H_m$  were obtained by nonlinear least squares fitting of Eq. 1 to thermal denaturation curves (monitored using CD at 234 nm). Protein concentrations used: 0.05 to 0.25 mg ml<sup>-1</sup>. Errors in measurements were ~1% for  $T_m$  and <10% for  $\Delta H_m$ . <sup>b</sup>  $T_m = T$  (in °C) where  $\Delta G_U = 0$ .

<sup>c</sup>  $\Delta T_m = T_{m,wt} - T_{m,mut}$  (in °C). <sup>d</sup>  $\Delta H_m =$  enthalpy of unfolding at  $T_m$  (in kcal mol<sup>-1</sup>).

<sup>e</sup>  $\Delta S_m = \Delta H_m/T_m$  (in cal mol<sup>-1</sup> K<sup>-1</sup>). <sup>f</sup>  $\Delta G_U$  values in kcal mol<sup>-1</sup> calculated using  $\Delta T_{m,wt-mut} \times \Delta S_{m,wt}$ .

$$\text{Eq. 1. } y = \frac{y_f + m_f [T] + y_u + m_u [T] \exp\left(\frac{-\Delta H_m \left(\frac{1}{T} + \frac{1}{T_m}\right)}{R}\right)}{1 + \exp\left(\frac{-\Delta H_m \left(\frac{1}{T} + \frac{1}{T_m}\right)}{R}\right)}$$

TABLE 2.  $\Delta(\Delta G)$  values for 32 Tyr to Phe mutants in eight proteins.

Protein	Mutant	%Buried	HB	$\Delta(\Delta G)_{obs}$	$\Delta(\Delta G)_{obs}$	$\Delta(\Delta G)_{HF}$	$\Delta(\Delta G)_{CE}$	$\Delta(\Delta G)/HB$
Human Lysozyme	Y20F	79.5	1	0.50		1.40	1.91	1.91
	Y38F	90.8	0		0.20	1.23	1.74	
	Y45F	68.2	0		-0.07	0.70	1.21	
	Y54F	88.6	1	1.01		2.01	2.52	2.52
	Y63F	20.8	0		0.23	0.47	0.98	
	Y124F	73.3	1	0.37		1.20	1.71	1.71
Phospholipase A2	Y52F	92.8	1	1.03		2.08	2.59	2.59
	Y73F	100.0	1	1.10		2.23	2.74	2.74
Human U1a RBP	Y13F	59.7	1	0.70		1.37	1.88	1.88
	Y31F	22	0		0.00	0.25	0.76	
	Y78F	80.9	1	0.00		0.91	1.42	1.42
	Y86F	99.9	1	2.60		3.73	4.24	4.24
RNase A	Y97F	100	1	3.54		4.67	5.18	5.18
RNase Ba	Y24F	100.0	1	0.02		1.15	1.66	1.66
	Y78F	100.0	1	1.35		2.48	2.99	2.99
	Y103F	88.5	1	0.00		1.00	1.51	1.51
RNase Sa	Y51F	86.5	1	2.18		3.16	3.67	3.67
	Y52F	100.0	1	3.44		4.57	5.08	5.08
	Y80F	80.1	1	1.51		2.42	2.93	2.93
	Y86F	88.5	1	0.36		1.36	1.87	1.87
RNase T1	Y11F	99.4	1	2.07		3.19	3.70	3.70
	Y42F	99.5	1	-1.15		-0.03	0.48	0.48
	Y56F	73.4	1	0.75		1.58	2.09	2.09
	Y57F	71.0	1	0.47		1.27	1.78	1.78
	Y68F	99.6	1	1.36		2.49	3.00	3.00
	Y27F	92.8	1	0.60		1.65	2.16	2.16
Staph Nuclease	Y54F	66.3	0		0.27	1.02	1.53	
	Y85F	36.9	1	0.00		0.42	0.93	0.93
	Y91F	100.0	2	2.14		3.27	3.78	1.89
	Y93F	91.0	1	1.61		2.64	3.15	3.15
	Y113F	-5.9	0		-0.20	-0.27	0.24	
	Y115F	23.9	0		-0.13	0.14	0.65	
	Average		81.7		1.15	0.11	2.16	2.67
Standard Deviation		16.5		0.86	0.13	0.92	0.92	0.92

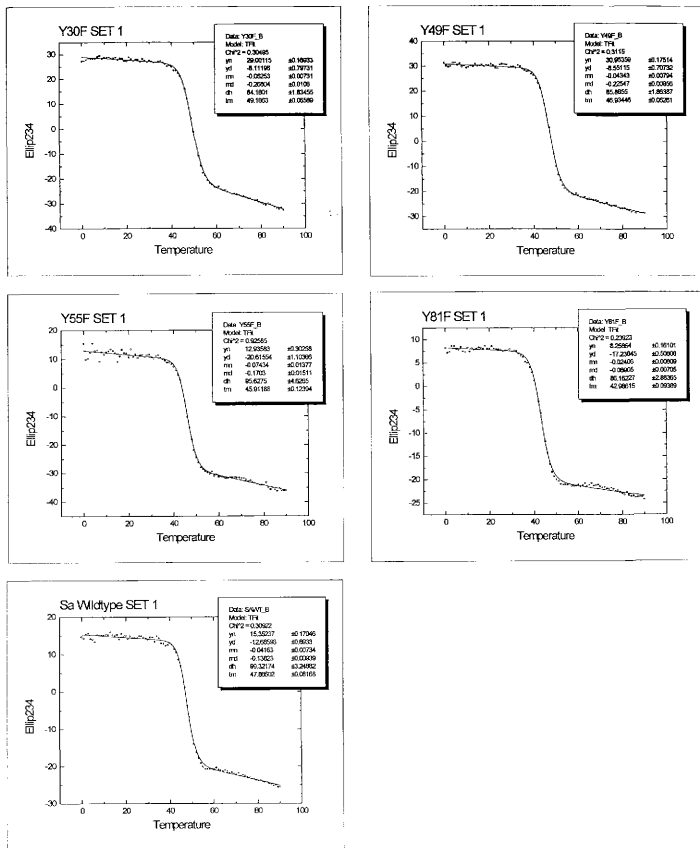


Figure 6. The thermal denaturation curves set-1 plotting the transition from the folded state to the unfolded state. A decrease in the stability of the mutant relative to wild type will cause the transition to unfolded to occur at a lower temperature.

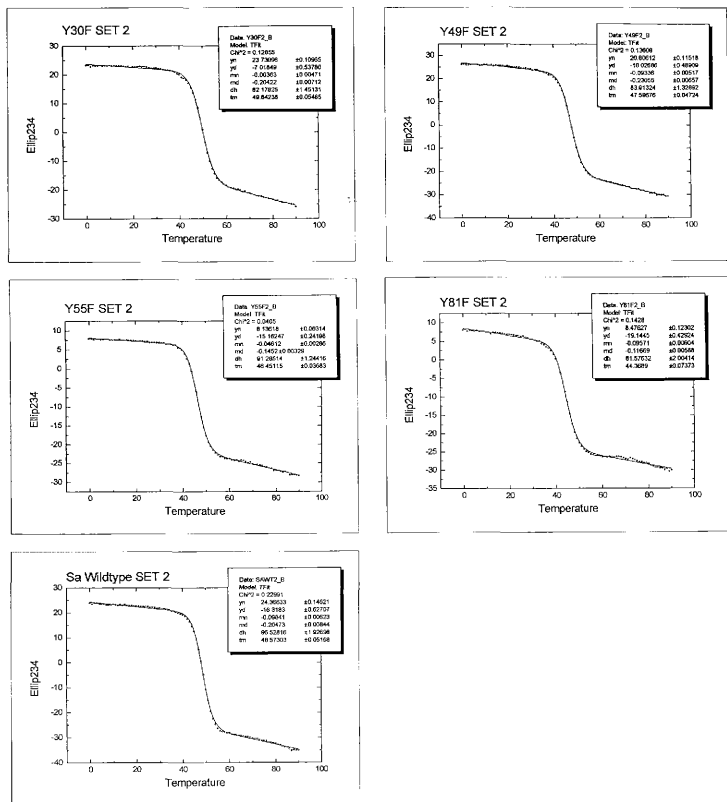


Figure 7. The thermal denaturation curves set-2 plotting the transition from the folded state to the unfolded state. A decrease in the stability of the mutant relative to wild type will cause the transition to unfolded to occur at a lower temperature.

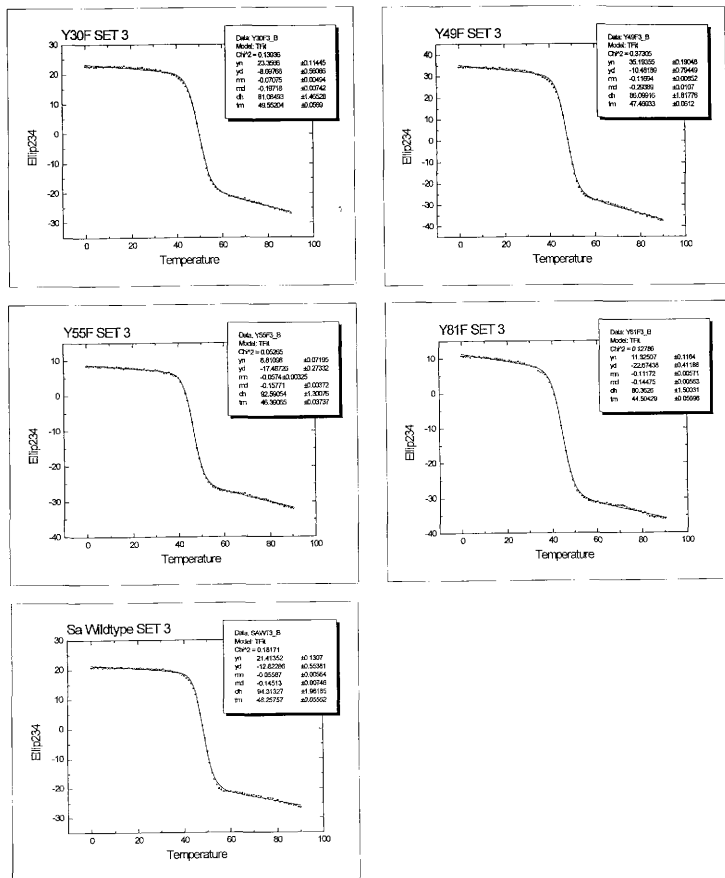


Figure 8. The thermal denaturation curves set-3 plotting the transition from the folded state to the unfolded state. A decrease in the stability of the mutant relative to wild type will cause the transition to unfolded to occur at a lower temperature.

## DISCUSSION

In the folded state, a protein's unique conformation is maintained by a combination of forces. Primarily, it occurs as a result of an aversion to mixing polar and apolar molecules. This causes the packing of hydrophobic side chains as far away from polar water as possible, leaving the remaining polar and neutral groups exposed to water (Pace, 1992). This results in a variety of structures, from rods to sheets to amorphous globs. The packing is very efficient in most proteins, and as a result of the proximity of many atoms to each other, attractive or electrostatic interactions occur between atoms of differing electron density. Naturally, an electron-dense atom is attracted to a less dense, or more positively charged atom and resists any attempt to break this interaction. As a result, atoms' distances are stabilized. Stability of this kind can be observed in Van der Waals interactions, salt bridges, or hydrogen bonding. A single bond of this type tends to be comparatively weak relative to the overall energy holding the protein together. However, these bonds are numerous, and in large numbers, contribute greatly to the stability of a conformation (Myers and Pace, 1996).

The force opposing the folded state is entropy. The observed orientation of a protein is just one of an enormous number that the chain of amino acids can form. Considerable energy must be taken out of the protein to fix it in a specific orientation. This flux of energy is balanced by the packing and electrostatic interactions mentioned above, and in most proteins the constructive and destructive energies nearly equal each other. This difference determines whether a protein is stable at a given temperature. This difference in free energy is called the conformational stability of the protein. If the packing and electrostatic forces are able to constrain the extra energy of movement in the amino acid chain, the protein is folded; if not, the chain unfolds (Pace, 1995.)

The major stabilizing electrostatic force in proteins is the hydrogen bond. Thermodynamic data provides substantial evidence that Tyr81 forms hydrogen bonds that contribute  $\sim 1.2$  Kcal/mol (Table-1) to conformational stability. The average  $\Delta G_U$  values on 36 hydrogen bonding Tyr  $\rightarrow$  Phe mutants in eight proteins is 1.15 Kcal/mol TABLE-2 (Pace, unpublished observations). Tyr81's  $\Delta G_U$  is near the mean for Tyr  $\rightarrow$  Phe mutants

suggesting it also forms an intramolecular bond or some equivalent imitative electrostatic interaction.

➤ Results from this study support the idea that intramolecular hydrogen bonds contribute to the conformational stability of RNase Sa.

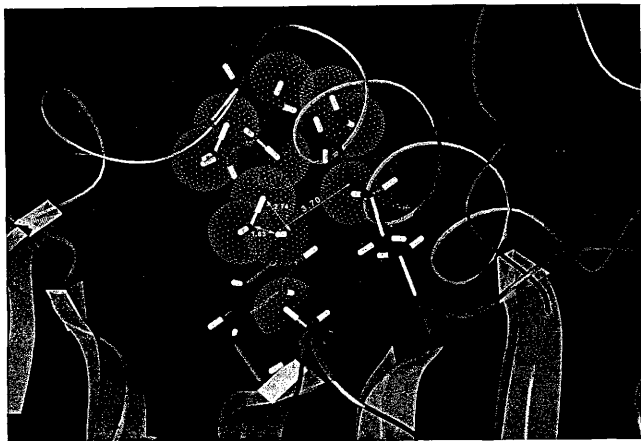


Figure 9 Details of the Y81F mutation site showing surrounding residues which may constrain the water molecule. Small dots representing Van der Waals radii are included to demonstrate the close proximity of the various structures, (rendered with Insight II).

The crystal structure for RNase Sa indicates Tyr81 forms either a 2.74Å hydrogen bond to a partially buried water molecule and/or an unusually long 3.7Å hydrogen bond to a nitrogen, Ne, on Arg68. The only other tyrosine in RNase Sa that forms an intramolecular bond over 3.00Å is Tyr86. This residue forms a 3.19Å intramolecular bond to Arg69 Ne with a  $\Delta G_{ij}$  of just 0.33 Kcal/mol, despite the shorter bond length.

➤ Results from this study support the idea that tyrosine hydrogen bonding strength can not simply be correlated to bond length, or geometry.



Figures-9, and Figure-10 are two different views depicting Tyr81's most likely electrostatic interactions. NMR results indicates Tyr81's phenolic proton has a well defined resonance at 9.28ppm which is typically considered good evidence that a proton forms an intramolecular bond (Laurents, unpublished observations). An interesting phenomena is that Tyr81's ring is continuously rotating at speeds of at least 10000Hz at room temperature. This spinning will generate a magnetic field that may influence local electrostatic interactions. Relative to intramolecular bonds, intermolecular bonds to surface water molecules appears to play a less important role in overall protein stability.  $\Delta G_0$  for Tyr 30, 49, 55 like previous Tyr mutant studies indicate that intermolecular bonds to surface water molecules can either slightly detract from or add to overall stability. Further study Tyr 30, 49, 55 and other mutants may enhance our understanding of the importance of protein hydration and its relation to protein stability.



Figure 10. Model of residues interacting with Tyr81. This blow-up depicts a 3.7 Å intramolecular bond between Tyr81 and Arg68 which acts as an acceptor. But as we see in this figure the local water molecule can also engage in hydrogen bonding, (rendered with Insight II).

### *Theoretical Molecular Analysis*

Figure-9 and Figure-10 both depict a 3.7 Å intramolecular bond between Tyr81 and Arg68 which acts as an acceptor. But as we see in this figure the local water molecule can also engage in hydrogen bonding. These images were created using the PDB x-ray crystal coordinate data sets with Biosym Technologies' Insight II (San Diego, CA) Biopolymer module. The C $\zeta$ -O $\eta$  bond of Tyr residues, have partial double bond characteristics; therefore, hydrogen atoms were sampled for hydrogen bonding interactions involving this sp<sup>2</sup> hybridized O $\eta$  atom with dihedral angles between 0 and 180°, in the plane of the phenyl ring. For added clarity, hydrogens were added to crystallographically resolved water molecules.

Intramolecular and intermolecular hydrogen bonds in the coordinate data sets were identified using the *hbonds* module of *pfis*. *hbonds* uses hydrogen bonding criteria derived from crystal studies of small molecules and is similar to criteria used in previous hydrogen bonding analyses. For each protein, hydrogen bonds were identified using the following steps 1). Distances between all potential donors and acceptors were evaluated. For a protein-protein hydrogen bonding pair, the pair is retained if the hydrogen atom to acceptor atom distance (HA distance) is < 3.8 Å. In protein-solvent hydrogen bonding pairs, two separate conditions were considered. For interactions in which the donated hydrogen is from the protein, a HA distance of < 2.6 Å is used, but for hydrogen bonding pairs in which the hydrogen is donated from a water molecule, a donor atom to acceptor atom (DA distance) of < 3.8 Å is used.

## CONCLUSION

Virtually every single thing that goes on our body is mediated by proteins, from hormone actions like insulin, to metabolism, digestion of food, to regulation of development – why a hand is a hand, why a foot is a foot. The molecules that are primarily responsible are proteins. When the folding process fails to work properly the consequences can be catastrophic. The list of diseases whose cause can be pinpointed to protein misfolding is growing almost daily, from cataracts to prion diseases to ankylosing spondylitis. And so we'd like to know how they fold up into these very exquisite three-dimensional structures that allow them to perform their functions.

By studying proteins, scientists hope to gain insight into how modifying the amino acid sequence might change their structure and stability. It is essential that we learn to predict how changes in amino acid sequences will affect the function, folding, and stability of proteins. The ability to either degrade or reinforce bonds and electrostatic forces opens up an enormous number of possibilities. The durability of proteins in their environment can be adjusted; a therapeutic drug's life span can be regulated, an industrial enzyme's usefulness can be strengthened for adverse conditions or photosynthesis can be made more efficient in plants by improving the ratio of carbon dioxide binding to oxygen binding. Altered properties might affect the efficiency of catalysis of a reaction or the transport of molecules. A combination of adjustments might then allow entirely new shapes and functions of proteins to be created. Once a protein's structure is known, it often is possible to deduce its function, which then tells scientists where to look for it in living organisms. A protein-folding model will further enhance rational drug design, where scientists will synthesize molecules to fit precisely where they can most effectively thwart disease. Theoretically, such drugs would be more effective and carry fewer side effects than conventional pharmaceuticals. This level of molecular sophistication requires an understanding of intramolecular interactions and the forces that contribute to the conformational stability of a protein.

## REFERENCES

- Anderson DE, Becktel WJ, Dahlquist FW. 1990. pH-induced denaturation of proteins: a single salt bridge contributes 3-5 kcal/mol to the free energy of folding of T4 lysozyme. *Biochemistry* 29:2403-2408.
- Anfinsen CB. 1973. Principles that govern the folding of protein chains. *Science* 181:223-230.
- Baker EN, Hubbard RE. 1984. Hydrogen bonding in globular proteins. *Prog Biophys Mol Biol* 44:97-179.
- Chothia CJ. 1984. Principles that determine the structure of proteins. *Annu Rev Biochem* 53:537-572.
- Dill KA. 1990. Dominant forces in protein folding. *Biochemistry* 29:7133-7155.
- Eckstein F, Schulz HH, Ruterjans H, Harr W, Maurer W. 1972. Stereochemistry of the transesterification step of ribonuclease T1. *Biochemistry* 11:3507-3512.
- Eriksson AE, Baase WA, Zhang X-J, Heinz DW, Blaber M, Baldwin EP, Matthews BW. 1992. The response of a protein structure to cavity-creating mutations and its relation to the hydrophobic effect. *Science* 255:178-183.
- Fersht AR, Shi JP, Knill-Jones J, Lowe DM, Wilkinson AJ, Blow DM, Brick P, Carter P, Waye MMY, Winter G. 1985. *Nature* 314:235-238.
- Feynman RP, Leighton RB, Sands M. 1977. *The Feynman Lectures on Physics*. Reading, MA: Addison Wesley Publishing Company.
- Findlay D, Herries DG, Mathias AP, Rabin BR, Ross CA. 1961. The active site and mechanism of action of bovine pancreatic ribonuclease. *Nature* 190:781-784.
- Gasperik, J., Prescakova, S., and Zelinka, J. (1982) *Biologia* (Bratislava) 37, 311 -381.
- Ho SN, Hunt HD, Horton RM, Pullen JK, Pease LR. 1989. Site-directed mutagenesis by overlap extension using the polymerase chain reaction. *Gene* 77:51-59.
- Kauzmann W. 1959. Some factors in the interpretation of protein denaturation. *Adv Protein Chem* 11:14-63.
- Kraulis PJ. 1991. MOLSCRIPT: a program to produce both detailed and schematic plots of protein structures. *J Appl Crystallogr* 24:946-950.

- Maitland GC, Rigby M, Smith EB, Wakeham WA. 1981. *Intermolecular Forces: Their Origin and Determination*. New York, NY: Oxford University Press.
- Miranker A, Radford SE, Karplus M, Dobson CM. 1991. Demonstration by NMR of folding domains in lysozyme. *Nature* 349: 633-6.
- Mirsky, A. E. and Pauling, L. 1936. *Proc Natl Acad Sci U S A* 22: 439-447.
- Myers JK, Pace CN. 1996. Hydrogen bonding stabilizes globular proteins. *Biophys J* 71:2033-2039.
- Pace CN. 1975. The stability of globular proteins. *CRC Crit Rev Biochem* 3:1-43.
- Pace CN. 1992. Contribution of the hydrophobic effect to globular protein stability. *J Mol Biol* 226:29-35.
- Pace CN. 1995. Evaluating contribution of hydrogen bonding and hydrophobic bonding to protein folding. *Methods Enzymol* 259:538-554.
- Pace CN, Laurens DV, Erickson RE. 1992. Urea denaturation of barnase: pH dependence and characterization of the unfolded state. *Biochemistry* 31:2728-2734.
- Pace CN, Shirley BA, McNutt M, Gajiwala K. 1996. Forces contributing to the conformational stability of proteins. *FASEB J* 76:75-83.
- Pauling L, Corey RB. 1951. The pleated sheet, a new layer configuration of polypeptide chains. *Proc Natl Acad Sci U S A* 37:251-256.
- Pauling L, Corey RB, Branson HR. 1951. The structure of proteins: two hydrogen-bonded helical configurations of the polypeptide chain. *Proc Natl Acad Sci U S A* 37:205-211.
- Perutz MF. 1979. Molecular adaptation in haemoglobin and thermophile bacteria. *Differentiation* 13:47-50.
- Prusiner SB. 1995. The prion diseases. *Sci Am* 48-57.
- Ramachandran, G. and Sassiékharan, V. 1968. Conformation of polypeptides and proteins. *Adv Protein Chem.* 23: 283-438.
- Scholtz JM, Marqusee S, Baldwin RL, York EJ, Stewart JM, Santoro M, Bolen DW. 1991. Calorimetric determination of the enthalpy change for the alpha-helix to coil transition of an alanine peptide in water. *Proc Natl Acad Sci U S A* 88:2854-2858.

- Sevcik J, Dauter Z, Lamzin VS, Wilson KS. 1996. Ribonuclease from *Streptomyces aureofaciens* at atomic resolution. *in press*
- Stickie DF, Presta LG, Dill KA, Rose GD. 1992. Hydrogen bonding in globular proteins. *J Mol Biol* 226:1143-1159.
- Tanford C. 1962. Contribution of hydrophobic interactions to the stability of the globular conformation of proteins. *J Am Chem Soc* 84:4240-4247.
- Uchida T, Egami F. 1967. Ribonuclease T1 from Taka-Diastase. *Methods Enzymol* 30:229-239.
- Umeyama H, Morokuma KJ. 1977. The origin of hydrogen bonding. an energy decomposition study. *J Am Chem Soc* 99:1316-1332.
- Zelinkova E, Bacova M, Zclinka J. 1971. Exocellular ribonuclease from *Streptomyces aureofaciens* II. properties and specificity. *Biochim Biophys Acta* 235:343-352.

All figures except figure 2 were created by John Bechert using Molscript, Insights II, Photoshop, Rasmol, and Excel